

Argonne National Laboratory

SYMPTOMS AND DETECTION OF A FISSION-PRODUCT RELEASE FROM AN EBR-II FUEL ELEMENT

Case 2. Defect below Fuel Elevation

by

R. M. Fryer, R. R. Smith,
E. R. Ebersole, and R. V. Strain

The facilities of Argonne National Laboratory are owned by the United States Government. Under the terms of a contract (W-31-109-Eng-38) between the U. S. Atomic Energy Commission, Argonne Universities Association and The University of Chicago, the University employs the staff and operates the Laboratory in accordance with policies and programs formulated, approved and reviewed by the Association.

MEMBERS OF ARGONNE UNIVERSITIES ASSOCIATION

The University of Arizona	Kansas State University	The Ohio State University
Carnegie-Mellon University	The University of Kansas	Ohio University
Case Western Reserve University	Loyola University	The Pennsylvania State University
The University of Chicago	Marquette University	Purdue University
University of Cincinnati	Michigan State University	Saint Louis University
Illinois Institute of Technology	The University of Michigan	Southern Illinois University
University of Illinois	University of Minnesota	The University of Texas at Austin
Indiana University	University of Missouri	Washington University
Iowa State University	Northwestern University	Wayne State University
The University of Iowa	University of Notre Dame	The University of Wisconsin

NOTICE

This report was prepared as an account of work sponsored by the United States Government. Neither the United States nor the United States Atomic Energy Commission, nor any of their employees, nor any of their contractors, subcontractors, or their employees, makes any warranty, express or implied, or assumes any legal liability or responsibility for the accuracy, completeness or usefulness of any information, apparatus, product or process disclosed, or represents that its use would not infringe privately-owned rights.

Printed in the United States of America
Available from
National Technical Information Service
U.S. Department of Commerce
Springfield, Virginia 22151
Price: Printed Copy \$3.00; Microfiche \$0.65

ARGONNE NATIONAL LABORATORY
9700 South Cass Avenue
Argonne, Illinois 60439

SYMPTOMS AND DETECTION OF
A FISSION-PRODUCT RELEASE
FROM AN EBR-II FUEL ELEMENT

Case 2. Defect below Fuel Elevation

by

R. M. Fryer, R. R. Smith,
E. R. Ebersole,* and R. V. Strain

EBR-II Project

(Case 1 was ANL-7605)

June 1970

*Idaho Facilities.

TABLE OF CONTENTS

	<u>Page</u>
NOMENCLATURE	6
ABSTRACT	7
I. INTRODUCTION.	8
II. DESCRIPTION OF EBR-II FUEL ELEMENT.	8
III. FISSION-PRODUCT MONITORING SYSTEMS.	9
A. Fission Gas Monitor (FGM).	9
B. Fuel Element Rupture Detector (FERD).	10
C. Radiometric Analyses of Cover-gas Samples	10
IV. CLASSIFICATION OF FISSION-PRODUCT RELEASES	11
A. Cladding Failure after Insertion in the Reactor.	11
B. Cladding Flaw Present before Insertion in the Reactor.	12
C. System of Classification.	13
V. CHRONOLOGY.	14
A. Run 32A.	14
B. Run 32B.	14
C. Runs 32C and 32D	16
D. Run 33A.	18
E. Run 33B.	19
F. Previous Irradiation History.	20
VI. POSTIRRADIATION EXAMINATION.	22
VII. SIZE OF SIGNAL FROM CLASS A, CASE 2 DEFECTS.	26
VIII. MATHEMATICAL MODELS OF THE XENON-135 BEHAVIOR.	29
A. Tramp Sources.	29
B. Class A, Case 2 Leakers	33
IX. SUMMARY	37
REFERENCES	38

LIST OF FIGURES

<u>No.</u>	<u>Title</u>	<u>Page</u>
1.	Cross Section of Mark-IA Driver-fuel Element	9
2.	Plot of ^{135}Xe Activity in Cover Gas at End of Run 32B, Showing Xenon Release after Pump Shutdown	15
3.	Xenon Activity at End of Run 32D, Showing a Small Release after Pump Shutdown.	17
4.	Plot of Portion of Run-33A Xenon Activity	19
5.	Run-33B Xenon Data, Showing Release from C2008 following Pump Shutdown on April 18, 1969	21
6.	Bond Traces for Defective Element E47 and Companion Element E45 from C2008	24
7.	Spade-to-Tube Weld on Defective Element E47, Showing Lack of Fill Weld.	25
8.	Lack of Fill Weld on Element E47 at 90° Clockwise from View in Fig. 7.	25
9.	Normal Spade-to-Tube Weld on Element E47 at 180° from View in Fig. 7	25
10.	Variation of Fission Rate, Pumped Coolant Pressure, and Relative Postshutdown Signal Size Radially across the EBR-II Core	27
11.	Comparison of Computed and Actual Tramp ^{135}Xe for the Startup and Shutdown of Run 37.	30
12.	Comparison of Run-32B Release from C2008 to Two Postulated Release Cases.	36

LIST OF TABLES

<u>No.</u>	<u>Title</u>	<u>Page</u>
I.	Failure Classification of Sodium-bonded EBR-II Metallic-fuel Elements	13
II.	Loading Changes after Run 32A.	14
III.	Loading Changes after Run 32B.	16
IV.	Loading Changes after Run 32C.	17
V.	Net Loading Changes between Runs 32D and 33A	18
VI.	Irradiation History of Subassembly C2008. . .	

NOMENCLATURE

A	Empirical power-decay parameter, hr^{-1}
k	Empirical power-decay constant, unitless
N	Atoms of given isotope
N_1	Atoms of ^{135}I
N_1^0	Atoms of ^{135}I remaining when postshutdown release stops
N_2	Atoms of ^{135}Xe
N_2^0	Atoms of ^{135}Xe remaining when postshutdown release stops
P	Pressure, $\text{lb}_f/\text{in.}^2$
ΔP	Pressure difference, $\text{lb}_f/\text{in.}^2$
Q	Fission-recoil release rate of a given isotope, atoms/sec
Q_0	Fission-recoil release rate of a given isotope, at full power, atoms/sec
r	Sodium leak rate, ml/sec
R	Ideal gas constant, $\text{atm-cc}/\text{g mole-}^\circ\text{R}$
t	Time, hr
Δt	Time difference, hr
t_{ps}	Time at which pump shutdown occurs, hr
T	Temperature, $^\circ\text{R}$
v	Bond-sodium volume in a driver element, ml
V	Gas volume, ml
λ_1	^{135}I decay constant, hr^{-1}
λ_2	^{135}Xe decay constant, hr^{-1}

SYMPTOMS AND DETECTION OF
A FISSION-PRODUCT RELEASE
FROM AN EBR-II FUEL ELEMENT

Case 2. Defect below Fuel Elevation

by

R. M. Fryer, R. R. Smith,
E. R. Ebersole, and R. V. Strain

ABSTRACT

Experience in EBR-II with a fuel element having a defect at the lower end has brought an increased ability to identify the type of defect by interpreting the response from fission-product monitors. The defect covered in this report became apparent when, during a reactor shutdown on December 24, 1968, a fission-product release occurred after pump shutdown. The source of leakage (subassembly C2008) was identified by correlating the timing of subsequent releases with routine changes in core loading. Before the identification was made, analysis had shown that the source must be a driver-fuel element with a defect near the lower end. This conclusion was confirmed by postirradiation examination.

The "fingerprint" of this particular type of leaker is easily distinguishable from that of releases through flaws at other elevations along a fuel element. This experience, coupled with experience from previous EBR-II leakers, has allowed a definition of failure types to be proposed. The character of the responses from the three fission-product monitoring systems is shown to be a function of the historical origin and the elevation of the flaw.

The irradiation of this type of leaker to 1.0 at. % burnup has provided further proof of the inherent safety in the design of the EBR-II fuel element. The safe operation of EBR-II was not compromised by the presence of this leaker in the core.

I. INTRODUCTION

Until May 1967, an understanding of potential fission-product releases in EBR-II was limited to theoretical studies.^{1,2} Since that time, the occurrence of a number of inadvertent fission-product releases has led to a practical evaluation of detection capabilities and an improved understanding of release mechanisms. So that other investigators might benefit from a knowledge of such releases, the pertinent information has been published.³⁻⁵

This report describes the fourth verified series of fission-product releases in EBR-II. The first series, beginning on May 24, 1967, was eventually traced to an encapsulated mixed-oxide element in experimental subassembly X011.³ The second, which occurred on November 23, 1967, and was not identified until May 1968, was eventually attributed to an encapsulated U-Pu-Zr metallic-alloy element in experimental subassembly X028.⁴

The third series of releases, in September 1968, marked the first verified cladding defect in an EBR-II driver-fuel element (in subassembly L462).⁵ The defect was located between the top of the fuel column and the upper end fitting of the element. The symptoms of the fission-product release from this type of cladding defect were shown to be entirely consistent with a physical model which permitted the intermittent exchange of bond sodium during reactor operation. No additional release was noted on reactor shutdown.

The fourth series--the one discussed in the present report--originated from a defect in the weld at the lower end fitting of an EBR-II driver-fuel element. For reasons discussed in detail below, the symptoms of such a release were observable only after the reactor and primary pumps had been shut down. Such behavior contrasted sharply with that noted for the failed element in subassembly L462.

As a result of this experience with two such widely differing types of releases, considerable progress has been made in understanding the symptoms and consequences of driver-element defects. We are now able to assess such releases on a quantitative, as well as qualitative, basis.

II. DESCRIPTION OF EBR-II FUEL ELEMENT

The discussion below of fission-product release mechanisms requires some previous explanation of the EBR-II Mark-IA fuel element. Details and dimensions are given in Fig. 1. The fuel portion of the element consists of a 13.50-in.-long by 0.144-in.-diam pin of uranium-5 wt % fission alloy enriched to 52.2 wt % ²³⁵U. The pin is contained in a Type 304 stainless steel jacket, or cladding, having an OD of 0.174 in. and an ID of 0.156 in. A sodium bond, which occupies the annulus separating the fuel material and

cladding, serves as a heat-transfer medium. Under room conditions (RTP), the level of the sodium bond is nominally 0.65 ± 0.15 in. above the fuel material. Above the sodium is a gas reservoir, 0.66 ml in volume, filled with argon. As burnup proceeds and the fuel swells, bond sodium is displaced upward, reducing the volume of the argon gas.

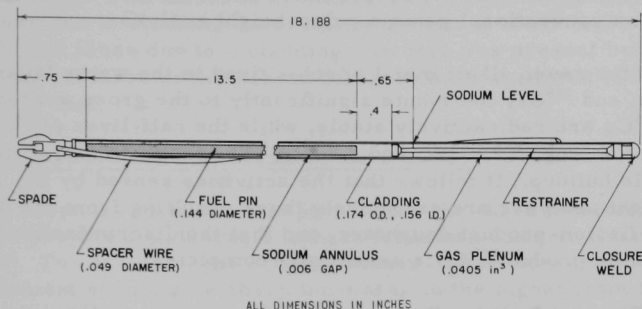


Fig. 1. Cross Section of Mark-IA Driver-fuel Element.
ANL Neg. No. ID-103-L5225 Rev. 1.

A restrainer plug, which limits longitudinal fuel growth, extends downward to within 0.40 in. of the fuel material. A spacer wire, 0.049 in. in diameter and helically wound around the cladding, spaces the elements in the subassembly and imparts rigidity to the fuel bundle.

III. FISSION-PRODUCT MONITORING SYSTEMS

Three monitoring systems are used to detect and annunciate the presence of fission products in the reactor's primary coolant and cover gas. Since these have been described in considerable detail elsewhere,⁶ only the most important features will be reviewed here.

A. Fission Gas Monitor (FGM)

In EBR-II, rare-gas fission products (krypton and xenon isotopes) are generated continuously through fissions in an ever-present, unavoidable contamination of core surfaces with fuel material. (This fuel material is referred to as "tramp uranium," and the associated xenon as "tramp xenon.") The rare-gas species found in the cover-gas plenum include ^{41}Ar , ^{87}Kr , ^{88}Kr , ^{89}Kr , ^{133}Xe , ^{135}Xe , and ^{138}Xe .

In the FGM, cover gas at a pressure of less than 5 psi and flowing at $80\text{--}90\text{ cm}^3/\text{min}$ is pumped through an electrostatic precipitation chamber, which contains a negatively charged traveling wire. Each of the rare-gas fission products is beta active, and at the instant of beta decay each of the

daughter species becomes a positively charged ion. Because of the electric field, the ionized species migrate to the traveling wire and become electronically neutralized. The wire carries the neutralized daughter species, now ^{87}Rb , ^{88}Rb , ^{89}Rb , ^{133}Cs , ^{135}Cs , ^{138}Cs , and ^{41}K , to a water layer in a downstream trap. All the above species are alkali metals and react chemically with the water. The activity level of the water layer is monitored continuously with a conventional gamma pulse-height analyzer.

Of the seven alkali metal species fixed in the water layer, only three, ^{88}Rb , ^{89}Rb , and ^{138}Cs , contribute significantly to the gross activity level. The ^{41}K and ^{133}Cs are radioactively stable, while the half-lives of ^{87}Rb and ^{135}Cs are much too long (5.2×10^{10} and 2.0×10^6 yr, respectively) to allow any perceptible buildup. It follows that the activities sensed by the gamma pulse-height analyzer are exclusively those resulting from the decay of rare-gas fission-product daughters, and that the discrimination against the activation product ^{41}Ar is essentially complete.

B. Fuel Element Rupture Detector (FERD)

In the FERD system, a stream of primary sodium coolant at approximately 700°F is pumped to the detection point by a dc electromagnetic pump. The sodium is taken from near the discharge side of the primary-secondary heat exchanger and is pumped through 2-in. Schedule-10 stainless steel pipe at 100 gpm.

Approximately 18 sec after leaving the core, the coolant flows through a 3-ft section of pipe completely surrounded by graphite moderator bricks. Located in the graphite stack are various neutron detectors, which monitor the neutron level of the coolant loop.

The system is designed to sense the presence of exposed fuel in the reactor within a few seconds following exposure. Application of this system to the failure-detection problem in sodium-cooled reactors has been discussed by Porges.⁷ It seems worth noting that no real signal has even been received on the FERD system from a defective fuel element. This system does, however, respond unambiguously to experimentally exposed fuel and to tramp uranium in the reactor.⁶

C. Radiometric Analyses of Cover-gas Samples

In the radiometric analyses of cover-gas samples, small samples of primary cover gas are taken periodically and analyzed for ^{133}Xe and ^{135}Xe . The samples consist of freshly flushed cover gas contained in standard 10-cm³ bulbs equipped at both ends with ground-glass stopcocks. Radiometric assays are conducted in calibrated and reproducible geometry with a precision 512-channel pulse-height analyzer. Activity levels for ^{133}Xe and ^{135}Xe are established by integrating the areas under the 81- and 250-keV photopeaks. The performance of the analyzer is periodically checked with the following sources: ^{65}Zn , ^{54}Mn , ^{137}Cs , and ^{235}U .

IV. CLASSIFICATION OF FISSION-PRODUCT RELEASES

This section discusses the response of the three monitoring systems to fission-product releases from driver-fuel elements, including an actual release and also potential types of releases that have not yet occurred in EBR-II. The releases are discussed under two primary categories: those due to cladding failure after insertion of the fuel element in the reactor, and those due to a cladding flaw that was present before insertion. Only releases of the second category have occurred to date in EBR-II driver fuel.

A. Cladding Failure after Insertion in the Reactor

The response or lack of response from the three monitoring systems should provide considerable inferential information on the nature of the release. For example, the sudden release of gas from the gas plenum of a fuel element should give sharp increases in the signal from the FGM and the levels of ^{133}Xe and ^{135}Xe in cover-gas samples, followed by simple radioactive decay. Because the index species for the FERD system are halogens and are fixed chemically in the sodium bond, the FERD system will not respond to a gas release.

All systems should respond, however, to a sudden release of bond sodium from a fuel element. In this case, halogen fission products enter the primary coolant system. The short-lived species such as ^{87}Br , ^{88}Br , ^{89}Br , ^{137}I , ^{138}I , and ^{139}I will be sensed by the FERD system. Some of the daughters of these species will be sensed by the FGM, whereas the daughters of longer-lived iodine fission products (namely ^{133}I and ^{135}I) will eventually be sensed in cover-gas samples. With these longer-lived products, the signals for ^{133}Xe and ^{135}Xe will not be sharp, but will build up to a maximum and then decay in accordance with the half-lives of the parent-daughter fission-product pairs.

The response or lack of response of the FERD system to a bond release may be used as a qualitative evaluation of the release rate. If the release rate is rapid (i.e., a substantial portion of the bond inventory is lost over a period of a minute or less), the FERD system will respond. If the release is gradual, however, the entry rate of delayed-neutron emitters may be too small for detection. In either event, the rare-gas daughters of the extruded halogen species will ultimately be sensed by the other monitoring systems.

The extent of burnup in the fuel material may affect the symptoms of the release. If the gas-plenum pressure is low (as for a fresh fuel element), primary sodium may actually be forced in through the defect and prevent the loss of bond sodium. Signals for such a situation would probably be small or nonexistent. If, however, the plenum pressure is high

(i.e., greater than 50 psia), bond sodium may be forced outward through the defect and give rise to significant signals.

Of even more importance in diagnosing the nature of a release is the behavior of the monitoring systems following reactor and primary-pump shutdown. The reduction in total coolant pressure following pump shutdown may cause an additional release of bond sodium through the defect. Since such a release occurs after the reactor is shut down, all short-lived halogen species will be absent. It follows that the FERD and FGM systems, which are sensitive to short-lived halogen species or their daughters, will fail to annunciate such a release. The method based on analyzing for ^{133}Xe and ^{135}Xe in the cover gas will apply, however, since these species are born from the decay of relatively long-lived halogen parents.

B. Cladding Flaw Present before Insertion in the Reactor

The above discussion was limited to the case of a fuel element that develops a flaw after insertion in the core. Let us now consider the actual experience with two fuel elements that were defective before insertion.

The fuel element from subassembly L462 was the first documented case of a fission-product release from an EBR-II driver element.⁵ The flaw was found to be a relatively large hole at an elevation above the top of the fuel and below the upper-end fitting. It now seems certain that plenum gas was lost, allowing primary sodium to backfill through the hole after insertion in the core. Presumably the backfilling occurred before reactor startup. The sealed upper portion of the gas plenum acted as a "diving bell" and limited the amount of sodium forced inward through the defect.

After the reactor was at power, fission products released by recoil action from the fuel surface diffused slowly upward through the bond to the flaw. But because the diffusion time was effectively longer than the half-lives of the shorter-lived halogen species, only the longer-lived iodine species such as ^{133}I and ^{135}I could reach the flaw and escape. Such a mechanism is entirely consistent with the facts that no FERD or FGM signal occurred, while, on the other hand, ^{133}Xe and ^{135}Xe signals were detected in cover-gas samples.

To explain what appeared to be a continuous extrusion of bond sodium, it was postulated that pressure fluctuations in the vicinity of the defect caused the intermittent release of bond sodium through the defect and the intermittent entry of primary coolant back through the flaw.⁵ The absence of evidence of a gas-type release was attributed to the fact that the sodium level with the pumps off was just above flaw elevation and, accordingly, mechanically prevented the escape of filling gas.

As described in Section VI, the defect responsible for the releases discussed in this report was also present at the time of insertion. In this case, however, the defect was located at the extreme lower region of the element. For a defect located in such a region, it seems certain that during pump startup primary sodium will be forced inward through the defect. Conversely, bond sodium will be forced outward on pump shutdown.

C. System of Classification

The foregoing discussion shows the feasibility of classifying the various types of defects according to whether the flaw was present before insertion in the core and where the flaw is located with respect to the fuel column. A flaw that was present before insertion will in this and subsequent reports be referred to as a Class A flaw. One that develops after insertion will be designated as a Class B flaw. Each of these categories is conveniently subdivided according to whether the flaw is above the fuel column (Case 1), below the fuel column (Case 2), or somewhere along the length of the fuel column (Case 3).

Table I describes the various classes and locations of flaws, along with the expected response of the monitors. Note that the responses listed in Table I apply strictly for relatively small defects. Large defects at any elevation can result in the release of the entire fission-product spectrum. However, the defects experienced to date have been small (a few mils or less) and in fact have been difficult to locate during postirradiation examinations.

TABLE I. Failure Classification of Sodium-bonded EBR-II Metallic-fuel Elements

Origin of Flaw	Elevation of Flaw	Expected Element Behavior and Monitor Response
Class A: Flaw Present before Insertion in Reactor	1. Above fuel column	Element backfills with sodium to just above the flaw upon insertion in reactor. Long-lived halogen fission products diffuse to the flaw, then pass through the flaw to the primary coolant. Xenon builds in, in accordance with the iodine-xenon half-lives during power operation. No FERD response, and slight, if any, FGM response.
	2. Below fuel column	Element backfills with sodium when pumps are on, then extrudes a packet of iodine-rich sodium following power and pump shutdown. Xenon builds in from the iodine, producing a hump in the normal tramp-xenon-decay curves. No FERD or FGM response.
	3. Along fuel column ^a	A medium or large flaw will release the entire spectrum of fission products to the coolant, since the total leak path is short (<21 mils). This will produce responses on all monitors during power operation. If the gas plenum communicates with the flaw, gas bubbles can produce step increases on the FGM and in cover-gas samples. A small flaw may inhibit the release of short-lived fission products, reducing the relative continuous FGM and FERD signals.
Class B: Flaw Opens after Insertion in Reactor	1. Above fuel column at gas-plenum elevation	Immediate FGM and cover-gas-sample signals are received. There is no FERD signal since the halogen species are fixed in the bond sodium. Pump shutdown can induce secondary bubbles. Pump restart may cause sodium backfilling, with the result that the element may subsequently act as a Class A, Case 1 above.
	2. Below fuel column	If the element is new, hence does not have significant gas-plenum pressure, no signal will be noted until pump shutdown, just as with Class A, Case 2 above. If high gas pressure is present, sodium will be forced out, possibly followed by gas bubbles (FGM and cover-gas-sample signals). Subsequent behavior cannot be predicted, since fuel meltdown may or may not occur.
	3. Along fuel column	Immediate FERD signal is received, followed by FGM and cover-gas-sample responses. If the plenum gas communicates, the FGM and cover-gas samples will undergo step rises; if not, the need for precursor decay will delay the responses.

^aThis case is academic and has been included for completeness only.

The behavior of the L462 releases⁵ clearly fall under the category of a Class A, Case 1 failure in the system described in Table I. In Sections V and VI, it will be shown that the releases described in the present report were characteristic of a Class A, Case 2 defect.

V. CHRONOLOGY

This section describes the sequence whereby the fission-product releases covered in this report were detected and identified as originating from subassembly C2008.

A. Run 32A

By the end of Run 32A (on December 17, 1968), subassembly L462 had been identified as the source of fission-product releases that began on September 9, 1968.⁵ Between Runs 32A and 32B, subassembly L462, along with a number of other subassemblies, was removed from the core. The net changes in loading following Run 32A are summarized in Table II.

TABLE II. Loading Changes after Run 32A

Core Position	Removed	Installed	Core Position	Removed	Installed
5D3	L462	L473	3B1	C2171	C2136
3D2	C2120	C2181	4E1	C2027	C2182
2D1	X000	C2008	3A2	C2167	X052

B. Run 32B

The reactor was started up on December 18, and after a scram and restart on December 19, operations continued without incident until December 24. During this period, the ^{135}Xe activity increased to and leveled off at $3.1 \times 10^{-3} \mu\text{Ci/ml}$, a value typical for the normal (tramp) background.

At 0903 on December 24, the reactor was inadvertently tripped, and at 1110 the primary pumps were secured (turned off). Under these circumstances, the expected behavior for ^{135}Xe was a normal radioactive decay. However, instead of decaying, the ^{135}Xe activity began to increase. After approximately 23 hr, the activity passed through a peak and then began to decay in accordance with the parent-daughter half-lives. The ^{135}Xe activity before, during, and after the shutdown is summarized in Fig. 2. As an illustration of the departure from normal behavior, the expected ^{135}Xe activity from the tramp sources has also been plotted. The subtraction of this component from the total measured activity defines the signal originating from the defective element.

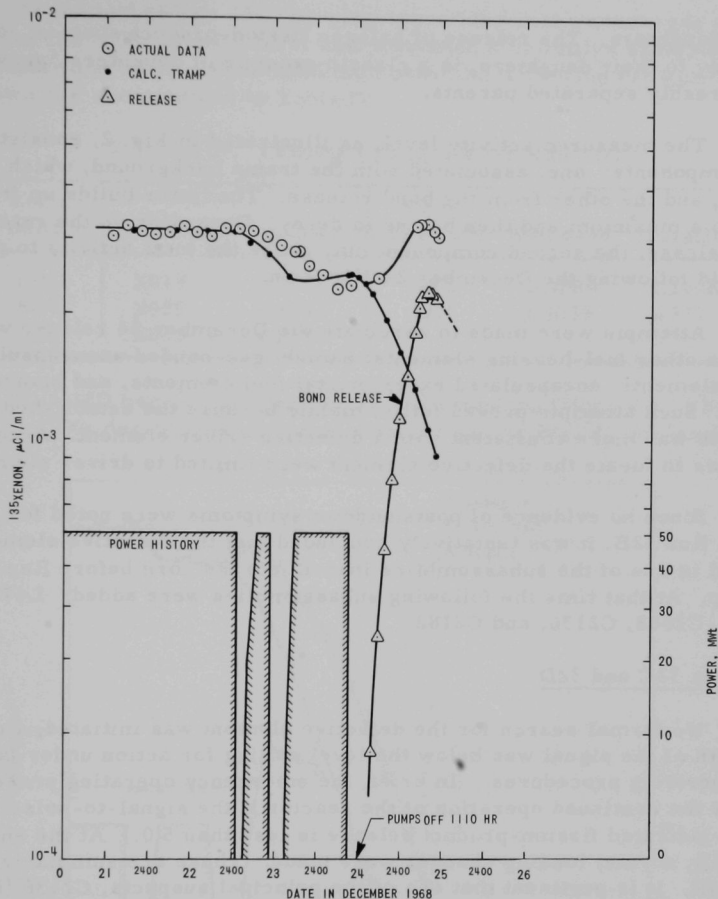


Fig. 2. Plot of ^{135}Xe Activity in Cover Gas at End of Run 32B, Showing Xenon Release after Pump Shutdown. ANL Neg. No. ID-103-M5369.

The increase in ^{135}Xe signal after primary-pump shutdown was immediately and correctly attributed to the release of bond sodium from a driver-fuel element with a defect in the vicinity of the lower-end fitting (spade). The mechanism explaining the ^{135}Xe behavior is as follows: During operation, the pressure component from the primary pumps tends to keep the sodium bond intact. In fact, under some circumstances, the pump pressure may actually force sodium into the element. Upon pump shutdown, the reduction in coolant pressure permits bond sodium to extrude through the defect. The bond contains significant amounts of bromine and iodine fission products, which subsequently decay to their respective krypton and

xenon daughters. The release of halogen fission-product species, followed by decay to their daughters, is a classic example of daughters "growing in" from freshly separated parents.

The measured activity level, as illustrated in Fig. 2, consists of two components: one, associated with the tramp background, which is decaying, and the other from the bond release. The latter builds up from zero to a maximum and then begins to decay. Depending on the rate of bond release, the second component may cause the total activity to peak, as it did following the December 24 shutdown.

Attempts were made to associate the December 24 release with defects in other fuel-bearing elements, namely gas-bonded unencapsulated oxide elements, encapsulated experimental fuel elements, and blanket elements. Such attempts proved futile, mainly because the established signal strength was more consistent with a defective driver element. Accordingly, attempts to locate the defective element were limited to driver elements.

Since no evidence of postshutdown symptoms were noted for runs before Run 32B, it was tentatively concluded that the defective element was located in one of the subassemblies loaded into the core before Run-32B startup. At that time the following subassemblies were added: L473, C2181, C2008, C2136, and C2182.

C. Runs 32C and 32D

No formal search for the defective element was initiated, since the strength of the signal was below the level calling for action under failed-fuel operating procedures. (In brief, the emergency operating procedures permit the continued operation of the reactor if the signal-to-noise ratio for an indicated fission-product release is less than 5.0.) At the end of Run 32B, normal loading changes were made. These are summarized in Table III. It is pertinent that one of the principal suspects, C2136 (installed just prior to Run 32B), was removed from the core after 32B.

TABLE III. Loading Changes after Run 32B

Core			Core		
Position	Removed	Installed	Position	Removed	Installed
3F1	C2148	C2167	4F1	C2174	C2168
5C2	C2116	C2148	3B1	C2136	C2171
3B2	C2147	C2116	3C2	X039	C2183
5A2	C2103	C2147	4B1	C2175	C2170

At the end of Run 32C, purging operations in the cover-gas system disturbed the ^{135}Xe activity level and prevented a definitive analysis of postshutdown activity. Fuel-handling operations following the Run-32C shutdown are summarized in Table IV.

TABLE IV. Loading Changes after Run 32C

Core Position	Removed	Installed	Core Position	Removed	Installed
6D2	X019	B3054	4F2	XA08	C2006
6B5	X020	B3002	6D1	B3039	A773
5E2	X033	C2010			

Run 32D began on December 28 and ended on January 2. The activity level for ^{135}Xe during this period is summarized in Fig. 3. An inspection of

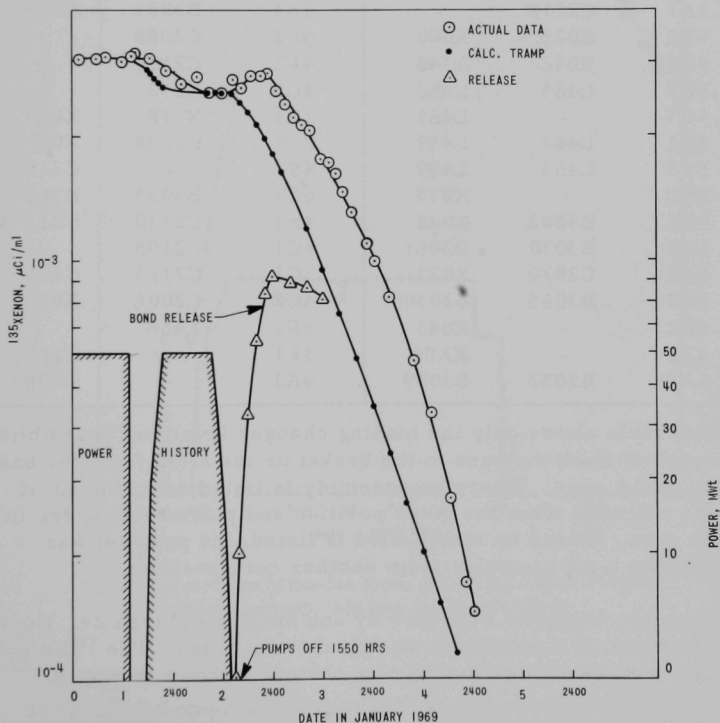


Fig. 3. Xenon Activity at End of Run 32D, Showing a Small Release after Pump Shutdown. ANL Neg. No. ID-103-M5370.

this figure shows that following the pump shutdown at 1550 on January 2, another fission-product release occurred. At this time, the reactor entered a scheduled 60-day shutdown for annual plant maintenance. Nothing of interest from the viewpoint of fission-product release occurred during this period.

D. Run 33A

Before the Run-33A startup, numerous loading changes were made. Fuel-handling operations are summarized in Table V. Note that subassembly C2008 was removed from the core during these loading changes.

TABLE V. Net Loading Changes between Runs 32D and 33A^a

Core			Core		
Position	Removed	Installed	Position	Removed	Installed
1A1	C2112	-	6A4	B3033	X055
4E2	X025	X000	5F2	C2088	-
7D5	X042	A748	4F3	C2119	-
5B3	L465	L460	4C3	X052	-
5C3	-	L461	2B1	X018	X057
5B1	L464	L459	2D1	C2008	X021B
5F3	L463	L499	4F1	-	C2184S
6D2	-	X019	6B3	B3034	B362
6B5	B3002	X020	4B1	C2170	C2175S
6E3	B3030	B3051	4C1	C2108	-
5E2	C2010	X033	3C1	C2163	C2065
6B2	B3065	B3057	4C2	C2006	X050
4D2	-	X043	5F1	L468	-
4F2	-	XA08	3F1	-	C2062
6A3	B3032	B3039	4A3	-	C2080

^aThis table shows only the loading changes involving assemblies removed from the core to the basket or installed from the basket to the core. Where no assembly is listed as removed, it was removed from the given position and placed elsewhere in the core. Where no installation is listed, the position was filled by a subassembly from another core position.

Run 33A began on February 27 and ended on March 29. During this run, no evidence of a postshutdown release was noted. The ¹³⁵Xe behavior following a pump shutdown during this period is shown in Fig. 4.

Of the list of suspect subassemblies remaining after Run 32D, subassemblies C2181, C2182, and L473 were in the core throughout Run 33A. Since no release was observed, these were eliminated as suspects. However,

C2008 had been removed from the core after Run 32D, when a release was noted, and was not, accordingly, in the core during Run 33A. By elimination, C2008 became the principal suspect.

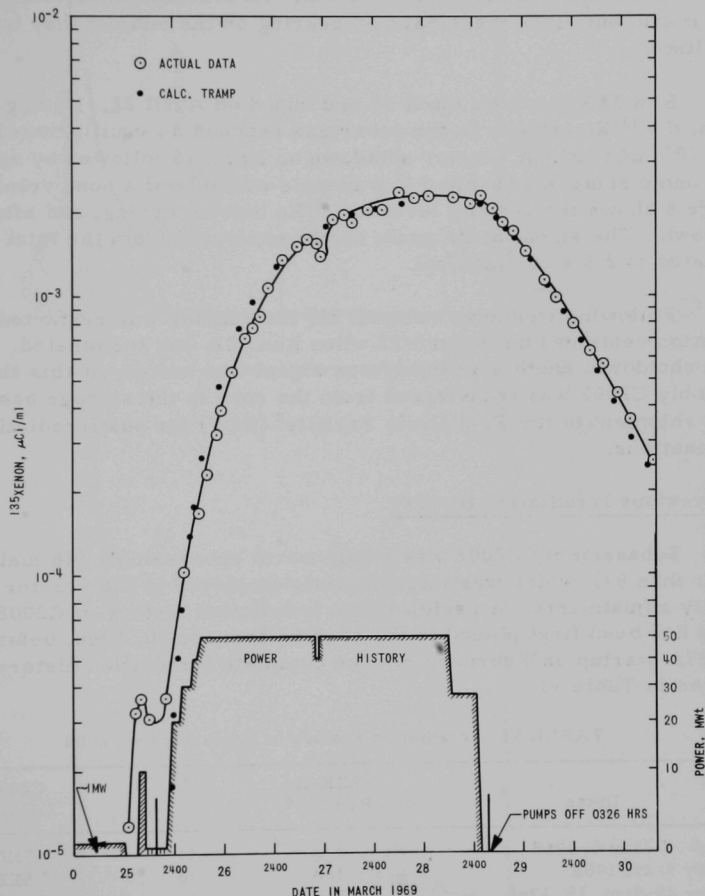


Fig. 4. Plot of Portion of Run-33A Xenon Activity (no release is evident during this shutdown). ANL Neg. No. ID-103-M5371.

E. Run 33B

It should be emphasized that formal search operations for the suspect were not carried out. However, with the suspect list reduced to one subassembly, C2008, attention was focused on proving the validity of the elimination process. Accordingly, C2008 was inserted in a row-3 position

before Run 33B to obtain a near-maximum, definitive signal. (Signal size as a function of core location is discussed in Section VII. The strength of the postshutdown signal is a function not only of flux, but of a radial coolant-pressure gradient.) Before Run-33B startup, other loading changes were made, but since these have no bearing on the subject they have not been listed.

Run 33B began on April 17 and ended on April 22. During the interim, the ^{135}Xe activity in the cover gas reached an equilibrium level of $2.3 \times 10^{-3} \mu\text{Ci/ml}$. A reactor shutdown on April 18 followed by an immediate pump shutdown resulted in a classic example of a bond release. Figure 5 shows the activity level for ^{135}Xe before, during, and after the shutdown. The signal at its peak, easily separated from the total level, amounted to $2.5 \times 10^{-3} \mu\text{Ci/ml}$.

Following shutdown on April 18, the reactor was restarted, and operation continued until April 22 when Run 33B was terminated. After pump shutdown, another unambiguous signal was noted. At this time, subassembly C2008 was transferred from the core to the storage basket to await shipment to the Fuel Cycle Facility⁸ (FCF) for postirradiation examinations.

F. Previous Irradiation History

Subassembly C2008 was a half-worth subassembly (46 fuel elements, rather than 91), which was intermittently employed in the reactor for reactivity adjustments. A review of the irradiation history of C2008 revealed that it had been first placed in the core on January 30, 1968, before the Run-27A startup on February 5. The complete irradiation history of C2008 is given in Table VI.

TABLE VI. Irradiation History of Subassembly C2008

Dates	EBR-II Run No. ^a		C2008 Location
Feb. 2-May 6, 1968	27A	to	3E2
May 9-27, 1968	28A	to	5E2
May 29-Sept. 15, 1968	28C	to	Storage basket
Sept. 17-25, 1968	30D	to	5E2
Sept. 30-Nov. 14, 1968	31A	to	Storage basket
Nov. 15-17, 1968	31G	to	4A1
Nov. 27-Dec. 17, 1968	32A	to	Storage basket
Dec. 18, 1968-Jan. 2, 1969	32B	to	2D1
Feb. 25-March 29, 1969	33A	to	Storage basket
April 7-22, 1969	33B	to	3E2
April 23, 1969	34A	to	Final removal

^aAll movements (i.e., locations) refer to the beginning of the listed run, not the end. For example, the last entry states that C2008 was removed from the core before the beginning of Run 34A.

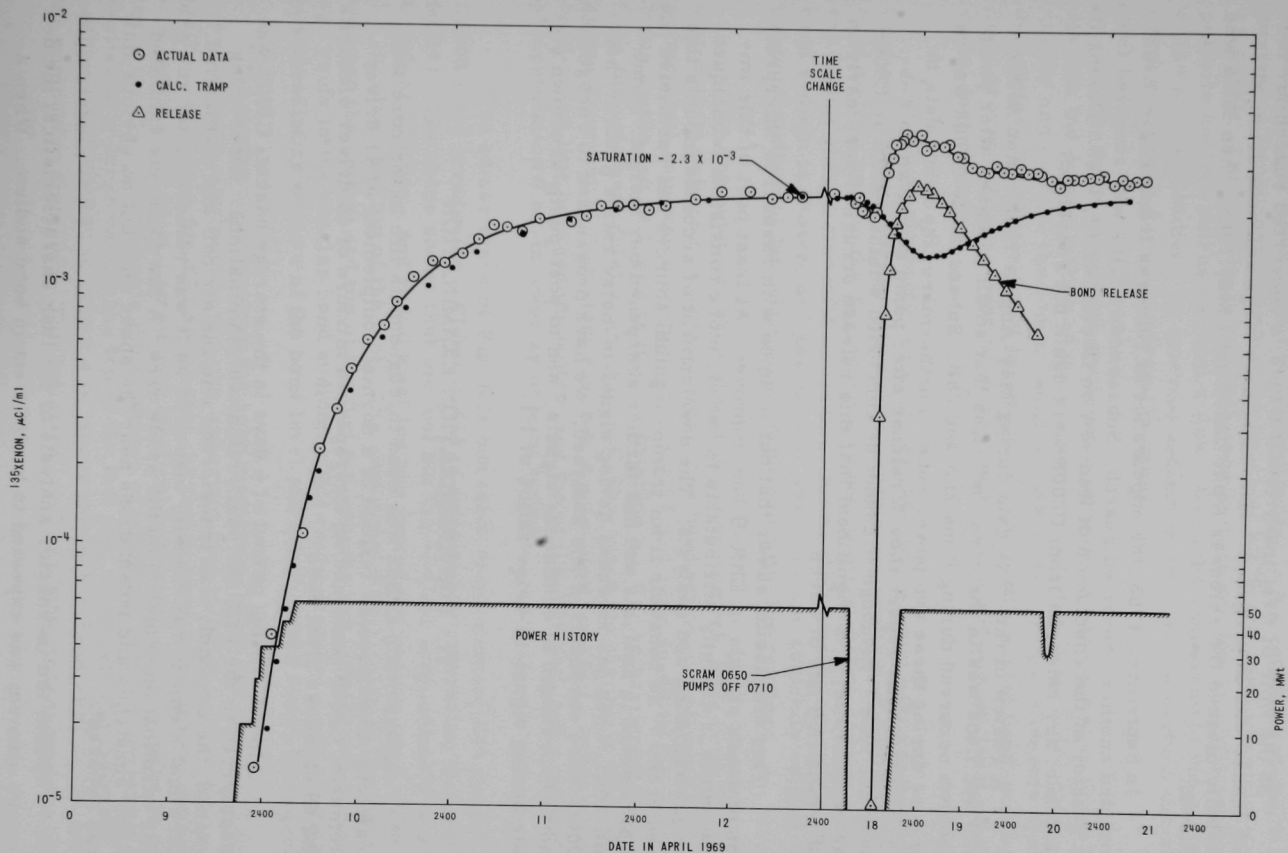


Fig. 5. Run-33B Xenon Data, Showing Release from C2008 following Pump Shutdown on April 18, 1969. ANL Neg. No. ID-103-M5372.

At the time of first insertion of C2008, a concerted search for the X028 leaker was in progress.⁴ The relatively large releases from X028 generally masked the releases from C2008 until May 1968, when X028 was removed.

In September 1968, the appearance of releases from leaker L462⁵ prompted another concerted search. Subassembly L462 was removed from the reactor at the conclusion of Run 32A on December 17, 1968. During its residence, any releases from C2008 were again not suspected.

A review of the ^{135}Xe data during May-August 1968, when neither X028 nor L462 was in the core, indicates that small releases after pump shutdown occurred during Runs 28A and 28B. Subassembly C2008 was in the core during these two power runs. Furthermore, the xenon data in Fig. 6 of the X028 report show a release after pump shutdown on February 29, 1968.⁴ Although it cannot be concluded whether X028 or C2008 was responsible, it is significant that this release occurred very early in the irradiation life of C2008.

This discussion shows that our acumen with respect to interpretation of xenon signals in EBR-II has improved. At least part of this improvement is directly attributable to better, more consistent techniques for gas sampling and analysis. The development of accurate models that predict the ^{135}Xe behavior from tramp-uranium sources has paralleled the improvement in analysis and has further sharpened our insight. Since mid-1967, when gas releases having signal-to-noise ratios greater than 1000:1 were encountered and analyzed,³ we have progressed to recognition and interpretation of continuous signals,⁵ and to post-pump-shutdown signals having signal-to-noise ratios of 1:1.

VI. POSTIRRADIATION EXAMINATION

Subassembly C2008 was used throughout its life in the core for reactivity adjustments. Instead of a normal complement of 91 driver elements, C2008 contained an interspersed mixture of 46 driver elements and 45 stainless steel rods.

After a cooling period of 6 days in the storage basket, C2008 was transferred to the FCF for postirradiation examinations. After being washed, the assembly was transferred into the air cell and dismantled.⁸ Each fuel element was visually inspected as it was removed from the grid. The examination centered on the spade area. A few elements exhibited slight scratches and indentations near the spade end, but no obvious flaw was apparent.

From the in-reactor analysis of the leak characteristics, the defective element was expected to be deficient in bond sodium. When a

subassembly is lifted from the storage basket in the reactor sodium, it experiences temporary external conditions of 700°F and approximately 12.5 psia. The combination of high temperature and low external pressure permits sodium extrusion from a flaw. When the subassembly rises clear of the primary sodium, no external sodium is available to backfill the element as it cools during the transfer operation.

The most important postirradiation examination based on this analysis was the determination of the sodium levels in the 46 fuel elements. The quality and level of the sodium bond of EBR-II driver-fuel elements are determined by eddy-current techniques.⁸ The eddy-current bond-test equipment provides a trace describing the bond quality and sodium level of individual fuel elements.

Of the 46 elements in C2008, 45 exhibited normal postirradiation bond qualities and levels. Normally, irradiation swelling of fuel displaces bond sodium up into the gas plenum, so that postirradiation sodium levels are higher than preirradiation levels. During the transfer operation, the bond sodium is frozen, and gas bubbles and voids are normally evident in the bond sodium of fuel elements discharged from the reactor.

The examinations showed that one fuel element, E47, from C2008, was clearly deficient in bond sodium. The bond traces for element E47 and an identical companion element from C2008 are reproduced in Fig. 6. The trace on the left of Fig. 6 is the one obtained for E47 before irradiation. (For fuel-element details, see Fig. 1.) This trace (on the left of Fig. 6) shows a normal 13.5-in.-long fuel pin, a good bond quality (a fairly straight bond-trace line between the bottom and top of the fuel pin), and a normal preirradiation 0.66-in. overlay of bond sodium.

The center trace of Fig. 6 is one taken from element E45 from C2008 after irradiation. Element E45 is an identical companion element to E47. The trace shows that the fuel pin has swelled longitudinally to a length of 13.65 in., and radial swelling has forced the sodium level up to 1.1 in. above the top of the fuel. The sine-wave-type ripples in the trace between the bottom and top of the fuel pin indicate gas bubbles and shrinkage voids in the annular bond sodium. This trace presents a quite normal postirradiation picture of the bond level and quality of an intact fuel element.

A comparison between the postirradiation traces for E45 and E47 reveals some similarities and one important dissimilarity. As to similarities, the trace for E47 shows that the fuel pin has swelled longitudinally to a length of 13.65 in., an amount identical to that for E45. Ripples in the trace for E47 also indicate the existence of voids and bubbles, including a particularly large void at the top of the fuel pin. However, the indicated sodium level for E47 is only 0.4 in. above the fuel instead of >1 in. as noted for companion elements. The indicated level of 0.4 in. corresponds to the

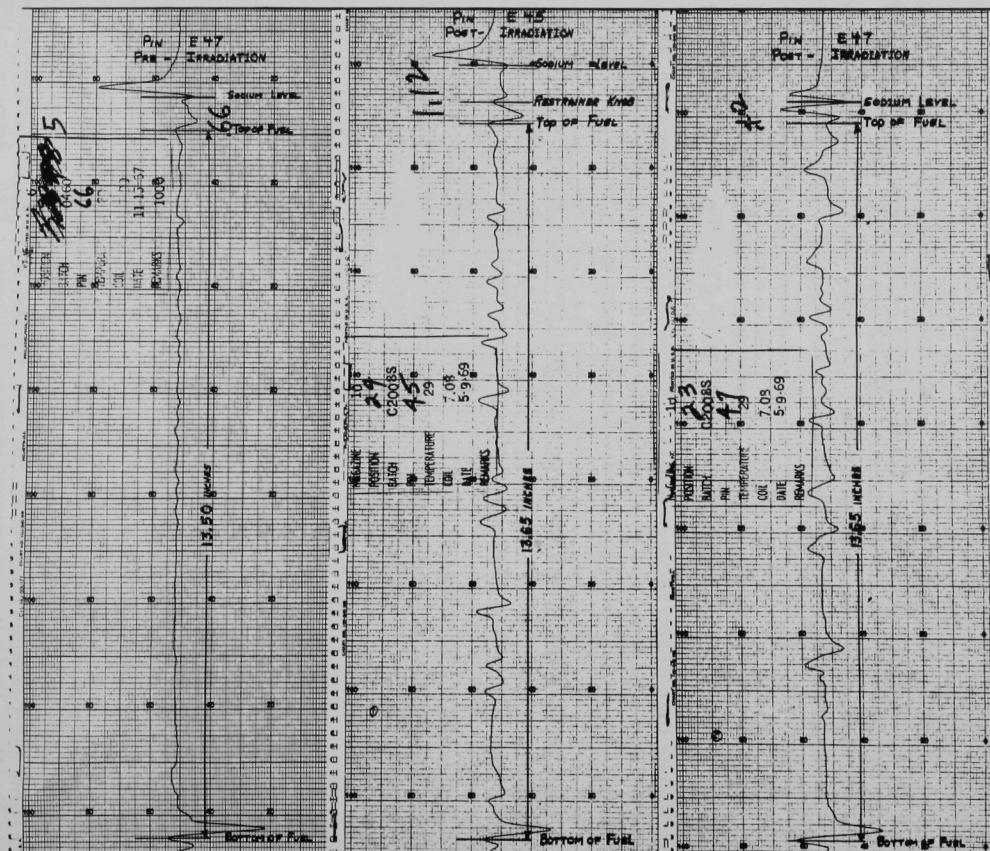


Fig. 6. Bond Traces for Defective Element E47 and Companion Element E45 from C2008. ANL Neg. No. ID-103-M5310.

level of the bottom of the restrainer (see Fig. 1) and may not be a true sodium level. It is probable that a small droplet of sodium adhered to the restrainer pin and that no continuum of sodium existed between the top of the fuel and the bottom of the restrainer. In any event, E47 was clearly deficient in bond sodium.

After the determination that E47 was deficient in bond sodium, this element was again visually inspected. The inspection revealed a very poor weld at the point at which the spade tip is attached to the lower element cladding. Figures 7 and 8 are enlarged photographs of the spade-to-cladding transition area. This area is normally filled with weld. Figures 7 and 8 show a general lack of fill weld at the edge of the cladding tube. Figure 9 shows the weld on the opposite side of E47. The weld here exhibits a normally smooth transition from the edge of the cladding tube to the spade.

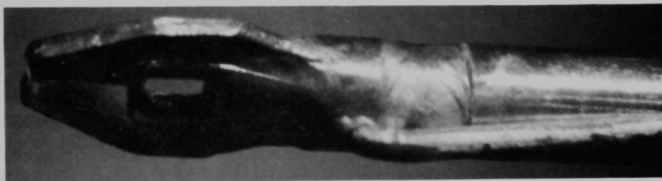


Fig. 7. Spade-to-Tube Weld on Defective Element E47, Showing Lack of Fill Weld. ANL Neg. No. ID-103-L5098.

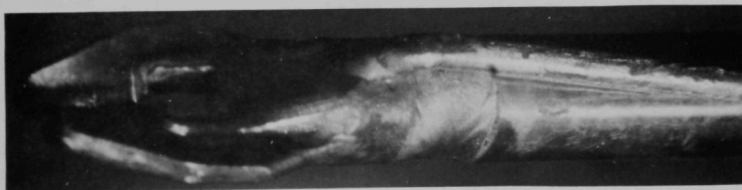


Fig. 8. Lack of Fill Weld on Element E47 at 90° Clockwise from View in Fig. 7. ANL Neg. No. ID-103-L5101.

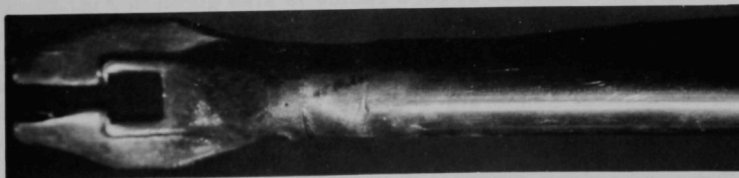


Fig. 9. Normal Spade-to-Tube Weld on Element E47 at 180° from View in Fig. 7. ANL Neg. No. ID-103-L5100.

During the jacket-assembly operation, poor weld-tip alignment resulted in only a partial circumferential seal weld between the cladding tube and the spade tip.

The upper end of the spade tip is essentially a press fit in the cladding tube (see Fig. 1). When the jacket was leak-checked at room temperature before element assembly, the partial weld and press fit probably prevented any leakage. Upon insertion in the reactor, the combination of high temperatures and pressure variations from pump operation allowed the leak path to open.

The examination of E47 demonstrated conclusively that fuel material neither slumped nor melted during its irradiation. In the classification given in Table I, the E47 defect is clearly of a Class A, Case 2 type.

VII. SIZE OF SIGNAL FROM CLASS A, CASE 2 DEFECTS

During Runs 34A through 36B in the period May to July 1969, another series of fission-product releases was noted. The source of these releases was not determined. Aside from magnitude, each release strongly resembled those from C2008. The magnitude of the maximum signal noted during this series ($1.1 \times 10^{-3} \mu\text{Ci/ml}$) was smaller than the maximum signal for C2008 ($2.5 \times 10^{-3} \mu\text{Ci/ml}$). This difference prompted a qualitative evaluation of the parameters that affect the size of signal from releases that occur after pump shutdown.

One obvious factor that affects the strength of the signal is the specific fission rate. Figure 10 shows the variation in specific fission rate as a function of core radius. From an arbitrary value of 1.0 at core center, the rate decreases to 0.65 at the core-blanket interface. Hence, the concentration of iodine fission products would be greatest in the bond of an element located in row 1.

Another important factor affecting the amplitude of the postshutdown signal is the pump pressure at the defect location. The variation in pump pressure as a function of core radius is also given in Fig. 10. Clearly, the amount of bond sodium released through a low-elevation defect upon pump shutdown will depend on the position of the subassembly in the core. After pump shutdown, all subassemblies, regardless of position, become subjected to identical temperature and pressure conditions at the spade end, i.e., 700°F and approximately 18 psia static pressure.

The bond sodium released through this type of defect has been in intimate contact with the fuel; essentially none of the release originates from the sodium that covers the top of the fuel pin. Accordingly, the sodium that extrudes will be representative of the bond in intimate contact

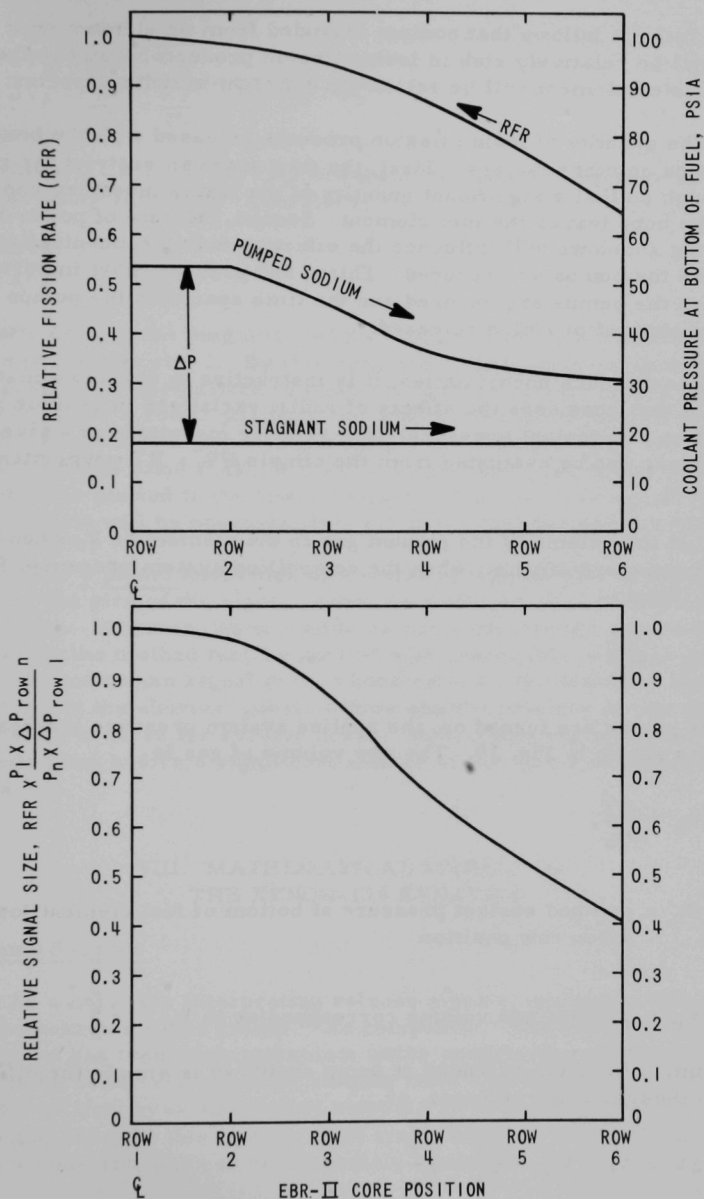


Fig. 10. Variation of Fission Rate, Pumped Coolant Pressure, and Relative Postshutdown Signal Size Radially across the EBR-II Core. ANL Neg. No. ID-103-M5652.

with the fuel. It follows that sodium extruded from an element near the core center will be relatively rich in iodine fission products, whereas the bond from an outer element will be relatively deficient in iodine species.

The quantity of iodine fission products released with the bond will also depend on other factors. First, the flaw size can restrict the release rate enough so that a significant quantity of the iodine inventory can decay before the bond leaves the fuel element. Second, the rate of power reduction during shutdown will influence the effective iodine concentration in the bond when the pumps are secured. Third, and perhaps most important, the time when the pumps are secured and the time span with the pumps off will affect the amount of iodine released.

Despite such uncertainties, it is instructive to develop a mathematical model that considers the effects of radial variations in reactor power distribution and coolant pressure. The relative magnitude of a given sodium release can be evaluated from the simple $PV = RT$ properties of the plenum gas.

Let the volume of the plenum gas in the element be V_0 when the coolant pumps are off, i.e., when the controlling system pressure, P_0 , is 18 psia. Then,

$$V_0 = \frac{RT}{P_0} \quad (1)$$

When the pumps are turned on, the applied system pressure increases to the values shown in Fig. 10. The new volume of gas is

$$V_n = \frac{RT}{P_n} \quad (2)$$

where

P_n = pumped coolant pressure at bottom of fuel element for a given row position

and

V_n = plenum-gas volume corresponding to P_n .

The volume of sodium extruded at pump shutdown is simply the difference between these two gas volumes, or

$$\Delta V = V_0 - V_n = \frac{RT}{P_0} - \frac{RT}{P_n} \quad (3)$$

The ratio of sodium volume released from an element in a given row n to that in a row-1 element is

$$\frac{\Delta V_n}{\Delta V_1} = \frac{\frac{RT}{P_0} - \frac{RT}{P_n}}{\frac{RT}{P_0} - \frac{RT}{P_1}} = \frac{P_1}{P_n} \frac{P_n - P_0}{P_1 - P_0}. \quad (4)$$

The terms $(P_n - P_0)$ and $(P_1 - P_0)$ are the ΔP values for the given row that occur at pump shutdown. Therefore,

$$\frac{\Delta V_n}{\Delta V_1} = \frac{P_1}{P_n} \frac{\Delta P_n}{\Delta P_1}. \quad (5)$$

This ratio defines the magnitude of the sodium release for a given row, relative to that for row 1. By this definition, the sodium release for a row-1 position is normalized to unity. If the fission rate is also normalized to unity for a row-1 position, the amount of iodine extruded from a defective element in a given row is simply the product of the relative fission rate and the ratio $P_1 \Delta P_n / P_n \Delta P_1$. The product gives the relative signal size, which is plotted in the lower portion of Fig. 10. The signal from a row-1 element will be approximately 2.5 times that for a row-6 element.

Since a priori knowledge of the size of a given flaw is not normally available, the size of the signal cannot, by itself, be used to identify the row position. However, when conditions are such that the maximum signal is achieved, the method may be applied with reasonable promise. To achieve the maximum signal from a bond release, the shutdown should be carried out in the shortest possible time and the primary pumps should be immediately secured for several hours. Such conditions allow the bond to begin extruding before a significant amount of the iodine inventory has decayed.

VIII. MATHEMATICAL MODELS OF THE XENON-135 BEHAVIOR

A. Tramp Sources

As a basis for interpreting release signals, one must first understand the behavior of the tramp ^{135}Xe component. The absolute ^{135}Xe level in the cover gas from tramp uranium under equilibrium conditions has proven to be relatively constant, ranging from approximately 2.5×10^{-3} to 3.5×10^{-3} $\mu\text{Ci/ml}$ over a period of months. Even more important, the buildup and decay of this isotope from tramp sources is smooth and reasonably consistent, and can be accurately predicted.

Models that predict the startup buildup of tramp ^{135}Xe have been presented in Ref. 5. This discussion will be limited to the shutdown equation for xenon behavior.

For this discussion let N_1 and λ_1 refer to ^{135}I , and N_2 and λ_2 refer to ^{135}Xe , where N is the number of atoms at any time and λ is the radioactive decay constant. The basis for development of the equation is that the concentration of ^{135}Xe is power-dependent.

The typical EBR-II shutdown is carried out at a rate that cannot exceed an outlet-temperature change of $2^\circ\text{F}/\text{min}$. To achieve this, the power is sometimes reduced by approximately 10 MW on a ramp; then a power hold is temporarily maintained to allow temperatures to stabilize (see power history in Fig. 11). This procedure is repeated until subcriticality

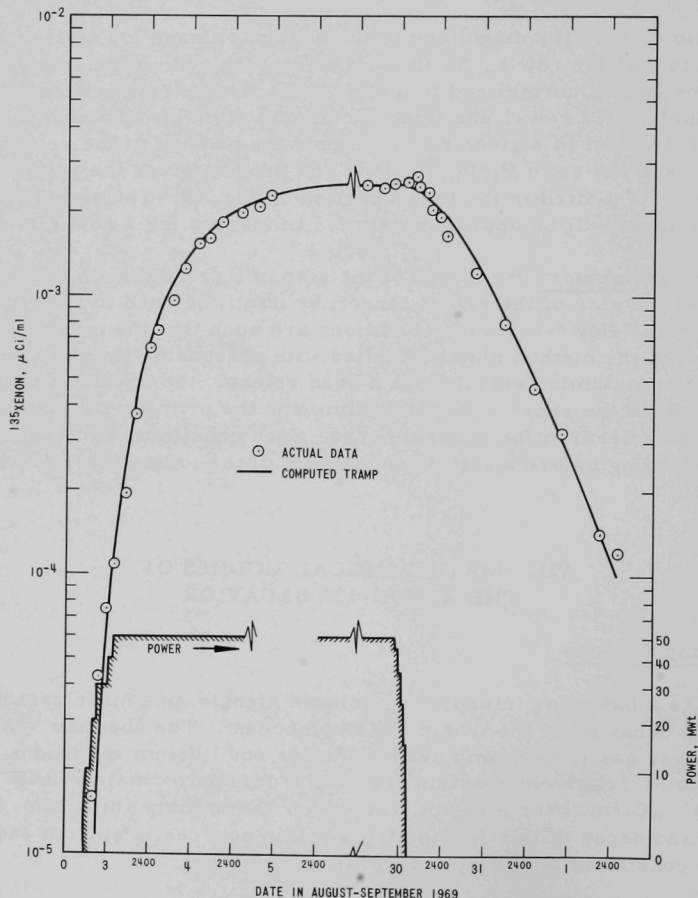


Fig. 11. Comparison of Computed and Actual Tramp ^{135}Xe for the Startup and Shutdown of Run 37. ANL Neg. No. ID-103-M5651.

is achieved. For such a shutdown, it is difficult to mathematically simulate ramp reductions followed by power holds. Rather, it is more convenient to time-smooth the shutdown power profile.

The time-smoothing can be simulated by assuming a source equation of the form

$$Q = Q_0 e^{-At}, \quad (6)$$

where

Q = fission-recoil release rate of ^{135}I at time t , atoms/sec,

Q_0 = fission-recoil release rate of ^{135}I at full power, atoms/sec,

t = time, hours, from the start of the shutdown,

and

A = empirical power-decay parameter, hr^{-1} .

Qualitative inspection of Eq. 6 shows that at

$$t_{\text{shutdown}} = 0, \quad Q = \frac{Q_0}{e^0} = Q_0 \text{ at full power,}$$

and

$$t_{\text{shutdown}} \rightarrow \infty, \quad Q = \frac{Q_0}{e^\infty} = 0 \text{ at zero power.}$$

Note that for this development, time is measured from the beginning of the shutdown. The differential equation describing the ^{135}I following the beginning of the shutdown is then

$$\frac{dN_1}{dt} = \text{fission-recoil release rate} - \text{decay rate}, \quad (7)$$

or

$$\frac{dN_1}{dt} = Q_0 e^{-At} - \lambda_1 N_1. \quad (8)$$

After integration, the equation describing ^{135}I during and after the shutdown is

$$N_1 = \frac{e^{-\lambda_1 t}}{\lambda_1} + \frac{Q_0}{\lambda_1 - A} (e^{-At} - e^{-\lambda_1 t}). \quad (9)$$

The differential equation describing the ^{135}Xe is simply

$$\frac{dN_2}{dt} = \text{formation rate} - \text{decay rate}, \quad (10)$$

or

$$\frac{dN_2}{dt} = +\lambda_1 N_1 - \lambda_2 N_2. \quad (11)$$

Equation 9 is substituted for N_1 in Eq. 11, and the result is integrated. Having thus described $N_2 = f(t)$, and having recognized that the decay rate (i.e., activity level) is $dN_2/dt = \lambda_2 N_2$, one obtains the desired final result,

$$\frac{dN_2}{dt} = e^{-\lambda_2 t} + \frac{\lambda_2(e^{-\lambda_1 t} - e^{-\lambda_2 t})}{\lambda_2 - \lambda_1} + \frac{Q_0 \lambda_1 \lambda_2 (e^{-At} - e^{-\lambda_2 t})}{(\lambda_1 - A)(\lambda_2 - A)} + \frac{Q_0 \lambda_1 \lambda_2 (e^{-\lambda_2 t} - e^{-\lambda_1 t})}{(\lambda_1 - A)(\lambda_2 - \lambda_1)}. \quad (12)$$

Definition of the empirical parameter A is still required. Since A must have the units of reciprocal time, it was assumed as a first approximation that A has the form

$$A = k/\Delta t, \quad (13)$$

where k is a constant and Δt is the time in hours required to bring the reactor down from full power to hot critical (50 kWt). Different values of k were assumed, and the calculated results of Eq. 12 were compared to some actual tramp ^{135}Xe decay curves. By this technique, it was concluded that

$$A = 0.8/\Delta t \quad (14)$$

gave an excellent fit to measured ^{135}Xe decay curves for both routine EBR-II shutdowns and scrams.

Actually, as may be apparent, Eq. 12 does not give the absolute xenon concentration in the cover gas; rather, it gives the fraction of saturation existing any time after the onset of shutdown. The calculated results are then normalized to the equilibrium ^{135}Xe concentration (when the reactor is at full power).

Equation 12 and the startup ^{135}Xe equations given in Ref. 5 have demonstrated repeatedly their capability for providing accurate, quantitative predictions of the tramp xenon as a function of time. A measure of the success in predicting the ^{135}Xe activity during the startup and shutdown of a typical operating segment may be inferred from Fig. 11. The ability

to predict the amplitude of the tramp ^{135}Xe at any given time forms the basis of a powerful method for concluding whether a release has occurred. It is a simple matter to subtract the predicted tramp from the gross activity. The difference, if significant, gives the signal from the fission-product release.

B. Class A, Case 2 Leakers

Because of the fluid mechanics involved in the release, the ^{135}Xe buildup from a bottom leaker cannot be described by a single, simple equation, as with the tramp source. When the pumps are shut off, the gas in the fuel-element plenum expands and forces iodine-rich bond sodium out. During this extrusion period, the introduction rate of ^{135}I varies for two reasons. First, the ^{135}I is decaying, and second, the rate of sodium extrusion decreases with time as the plenum-gas pressure approaches the existing external pressure. For most leakers, the release probably attains pressure equilibrium and stops. Alternatively, if the pumps are turned back on, the flow of sodium across the flaw reverses and effectively prevents the ^{135}I release.

In either case, there is a discontinuity in the introduction of ^{135}I into the primary tank. During the extrusion period, the ^{135}Xe builds in from ^{135}I being continuously, although not uniformly, released to the primary tank. When the release stops, ^{135}I is no longer released to the coolant. At this time, it is convenient to separate the ^{135}Xe from the bond into two components: one which is present at the time the bond release stops and which continues to decay; and the other which grows in from the residual released inventory of ^{135}I .

Consider the bond sodium in the fuel element. During the power shutdown, ^{135}I in the bond is decaying, and the release of the sodium does not start until the pumps are shut off. Equation 9 exactly describes the decay of ^{135}I in the bond before the leak begins. The only notation required is that Q now refers to a fuel pin, rather than tramp uranium. This equation is therefore the starting point for describing the release.

With the pumps shut off, the entry rate of ^{135}I into the primary sodium is

$$\frac{rN_1}{v} \text{ atoms/sec} \quad (15)$$

where

r = sodium leak rate, ml/sec,

N_1 = atoms of ^{135}I in the bond sodium,

and

v = volume of bond sodium, ml.

From Eq. 15, the differential equation describing the time rate of buildup of ^{135}I may be derived; thus,

$$\frac{dN_1'}{dt} = \text{introduction rate} - \text{decay rate}, \quad (16)$$

or

$$\frac{dN_1'}{dt} = \frac{rN_1}{v} - \lambda_1 N_1'. \quad (17)$$

Here a prime has been added to the N_1 to distinguish between the N_1 in the bond sodium and the N_1' being released to the primary sodium. As noted, N_1 in Eq. 17 is given by Eq. 9. Introduction of Eq. 9 into Eq. 17 and integration yield

$$N_1' = \frac{r}{v} \left\{ \left[\frac{te^{-\lambda_1 t}}{\lambda_1} + \frac{Q_0}{\lambda_1 - A} \left(\frac{e^{-At}}{\lambda_1 - A} - te^{-\lambda_1 t} \right) \right] - \left[\frac{t_{ps}}{\lambda_1} + \frac{Q_0}{\lambda_1 - A} \left(\frac{e^{(\lambda_1 - A)t_{ps}}}{\lambda_1 - A} - t_{ps} \right) \right] e^{-\lambda_1 t} \right\}. \quad (18)$$

Equation 18 describes the buildup of ^{135}I atoms in the primary sodium from the leaker, but only during the period that the leak is actually in progress. The condition that $N_1' = 0$ at $t = t_{ps}$ was used as an initial boundary condition. The time t_{ps} is the time of pump shutdown, measured from the time of the start of power shutdown. In the equation, t_{ps} is a constant, not a variable.

Once the leak starts, ^{135}Xe builds in as the released ^{135}I decays. The differential describing this buildup is

$$\frac{dN_2}{dt} = \text{formation rate} - \text{decay rate}, \quad (19)$$

or

$$\frac{dN_2}{dt} = \lambda_1 N_1' - \lambda_2 N_2, \quad (20)$$

where N_1' is described in Eq. 18. Substitution of Eq. 18 into Eq. 20 and integration yield the desired result,

$$\begin{aligned} \frac{dN_2}{dt} = & \frac{r\lambda_1\lambda_2}{v} \left(\frac{[(\lambda_2 - \lambda_1)t - 1]e^{-\lambda_1 t}}{\lambda_1(\lambda_2 - \lambda_1)^2} + \frac{Q_0}{\lambda_1 - A} \left\{ \frac{e^{-At}}{(\lambda_1 - A)(\lambda_2 - A)} \frac{[(\lambda_2 - \lambda_1)t - 1]e^{-\lambda_1 t}}{(\lambda_2 - \lambda_1)^2} \right\} \right. \\ & - \frac{t_{ps}e^{-\lambda_1 t}}{\lambda_1(\lambda_2 - \lambda_1)} - \frac{Q_0}{\lambda_1 - A} \left[\frac{e^{(\lambda_1 - A)t_{ps}}e^{-\lambda_1 t}}{(\lambda_1 - A)(\lambda_2 - \lambda_1)} - \frac{t_{ps}e^{-\lambda_1 t}}{\lambda_2 - \lambda_1} \right] \Bigg) - \frac{\lambda_1 r\lambda_2}{v} \left(\frac{[(\lambda_2 - \lambda_1)t_{ps} - 1]e^{(\lambda_2 - \lambda_1)t_{ps}}}{\lambda_1(\lambda_2 - \lambda_1)^2} \right. \\ & + \frac{Q_0}{\lambda_1 - A} \left\{ \frac{e^{(\lambda_2 - A)t_{ps}}}{(\lambda_1 - A)(\lambda_2 - A)} - \frac{[(\lambda_2 - \lambda_1)t_{ps} - 1]e^{(\lambda_2 - \lambda_1)t_{ps}}}{(\lambda_2 - \lambda_1)^2} \right\} - \frac{t_{ps}e^{(\lambda_2 - \lambda_1)t_{ps}}}{\lambda_1(\lambda_2 - \lambda_1)} \\ & \left. - \frac{Q_0}{\lambda_1 - A} \left[\frac{e^{(\lambda_2 - A)t_{ps}}}{(\lambda_1 - A)(\lambda_2 - \lambda_1)} - \frac{t_{ps}e^{(\lambda_2 - \lambda_1)t_{ps}}}{\lambda_2 - \lambda_1} \right] \right) e^{-\lambda_2 t}. \end{aligned}$$

This result was derived with the boundary condition that $N_2 = 0$ at $t = t_{ps}$. Note that this equation also applies only during the period that the leak is in progress, and that Q_0 refers to the fission-recoil release rate from a fuel pin. When the leak stops, Eq. 18 can be solved for the ^{135}I atoms that have been introduced into the primary tank but have not decayed. Division of the right-hand side of Eq. 21 by λ_2 (from $dN_2/dt = \lambda_2 N_2$) will convert Eq. 21 to the form $N_2 = f(t)$. Solution of that equation at the time the leak stops defines the quantity of ^{135}Xe in the primary tank from the leak.

At this point, the ^{135}Xe (N_2) atoms present simply decay according to the equation

$$N_2 = N_2^0 e^{-\lambda_2 t}, \quad (22)$$

where

$$N_2^0 = \text{atoms of } ^{135}\text{Xe} \text{ left when leak stops}$$

and

$$t = \text{time, measured from the point at which the leak stopped.}$$

The relationship

$$N_2 = \frac{\lambda_1 N_1^0}{\lambda_2 - \lambda_1} (e^{-\lambda_1 t} - e^{-\lambda_2 t}) \quad (23)$$

defines the quantity of ^{135}Xe being produced from the ^{135}I left when the leak stops, where

$$N_1^0 = \text{atoms of } ^{135}\text{I} \text{ left when leak stops}$$

and

$$t = \text{time, measured from the point at which the leak stopped.}$$

Summation of the results from Eqs. 22 and 23 yields the total number of ^{135}Xe atoms at the given time.

These equations have been applied on an absolute basis to define the shape and magnitude of a postshutdown release. However, some assumptions must be made to initiate the calculation. Since the leak rate r is not known, it must be estimated. From the mechanical design of the fuel element, one can estimate the total amount of sodium that can be extruded. This estimate is based on the $PV = RT$ properties of the plenum gas and the system volumes. The leak rate is simply the volume of extruded sodium distributed over an assumed period of time. The absolute release

rate of recoil fission products, Q_0 , can be calculated on an average basis with reasonable accuracy from the results of exposed-fuel calibration studies conducted in EBR-II.⁶

The terms λ_1 , λ_2 , v , A , and t_{ps} are all known constants. With the number of atoms of ^{135}Xe known as a function of time, the activity in curies is given from the relationship

$$\text{Activity} = \frac{\lambda_2 N_2}{3.7 \times 10^{10}}. \quad (24)$$

The curie value is divided by the volume of the reactor cover gas at operating temperature, $2 \times 10^7 \text{ cm}^3$, to convert the results to the same units as those used in cover-gas analyses.

These equations, in somewhat simplified form, were used to generate the data shown in Fig. 12. In this figure, curve 1 was generated from the assumption that the entire bond of a single fuel element leaked very

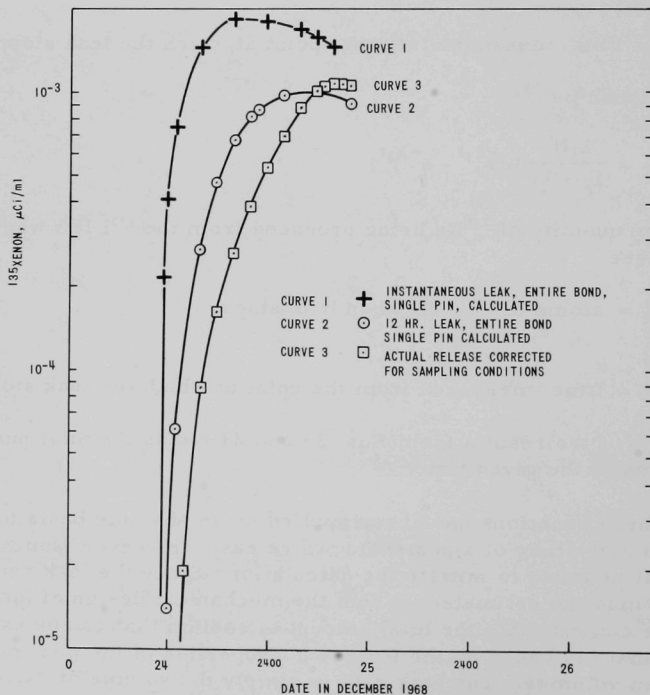


Fig. 12. Comparison of Run-32B Release from C2008 to Two Postulated Release Cases. ANL Neg. No. ID-103-M5374.

rapidly. Since a rapid leak carries out a maximum inventory of ^{135}I at the earliest possible time, it should produce more ^{135}Xe and the buildup rate should be more rapid than that from a slower leak. This is apparent in comparison with curve 2, which was calculated from the assumption that the entire bond of a single pin leaked over a 12-hr period. Curve 3 is the actual release data for the December 24, 1968 release in Run 32B (Fig. 2). The data of curve 3 have been corrected to account for the sampling procedure used. This correction converts the sample-measurement conditions, 70°F and 1 atm, to actual reactor cover-gas conditions, 700°F and 1 atm.

Although the comparison is not perfect, it is qualitatively correct. A more disciplined application of the equations derived in this section should result in an even better model. Perhaps the only questionable practice in the application of these equations is the need for estimating the leak rate r and the implicit assumption that r is constant with time.

IX. SUMMARY

The operation of EBR-II has continued to provide important information concerning the safety implications of operating with defective fuel elements. The information presented in this report is considered reassuring, since the defective element involved achieved a burnup of approximately 1.0 at. % in various core positions without any further deterioration of fuel or cladding. Furthermore, the fission-product releases from the element were innocuous and in no way affected the operation of the reactor plant. The safe operation of the EBR-II was at no time compromised by the presence of this leaker in the core.

This type of leaking element has a clear, distinguishable fingerprint. The fingerprint appears as a hump on the smooth xenon-decay curves after power and pump shutdown. Mathematical models of the startup and shutdown behavior of xenon sources have been developed and demonstrated to be accurate. These provide a firm knowledge of the time-dependent behavior of xenon isotopes in the cover gas. Such knowledge permits the positive annunciation of this specific type of defect.

Experience with this element and with previous releases³⁻⁵ has led to a definition of types of fission-product releases. The definition specifies the response expected from the three EBR-II monitoring systems as a function of the elevation and the historical origin of the flaw in the given element. As more experience is gained, even clearer specifications of the responses of the various monitors to a given failure type should be possible.

REFERENCES

1. L. J. Koch, H. O. Monson, D. Okrent, M. Levenson, W. R. Simmons, J. R. Humphreys, J. Haugsnes, V. C. Jankus, and W. B. Loewenstein, *Hazard Summary Report: Experimental Breeder Reactor II (EBR-II)*, ANL-5719 (May 1957).
2. L. J. Koch, W. B. Loewenstein, and H. O. Monson, *Addendum to Hazard Summary Report: Experimental Breeder Reactor II (EBR-II)*, ANL-5719 (Addendum) (June 1962).
3. R. R. Smith, D. W. Cissel, C. B. Doe, E. R. Ebersole, and F. S. Kirn, *Locating and Identifying the Source of the May 24, 1967, Fission-product Release in EBR-II*, ANL-7543 (April 1969).
4. R. R. Smith, E. R. Ebersole, R. M. Fryer, and P. B. Henault, *Origin of Fission-product Releases in EBR-II, November 23, 1967 to May 6, 1968*, ANL-7604 (May 1970).
5. R. M. Fryer, E. R. Ebersole, P. B. Henault, and R. R. Smith, *Symptoms and Detection of a Fission-product Release from an EBR-II Fuel Element: Case 1. Defect above Fuel Elevation*, ANL-7605 (Jan 1970).
6. R. R. Smith, C. B. Doe, and E. R. Ebersole, *Exposed-fuel Calibration Studies in EBR-II: Second Series*, ANL-7558 (Jan 1970).
7. K. G. A. Porges, *Fuel-failure Detection in LMFBR Power Plants*, ANL-7533 (Feb 1969).
8. J. C. Hesson, M. J. Feldman, and L. Burris, *Description and Proposed Operation of the Fuel Cycle Facility for the Second Experimental Breeder Reactor (EBR-II)*, ANL-6605 (April 1963).

ARGONNE NATIONAL LAB WEST



3 4444 00007901 2

X

